Talanta 99 (2012) 1057–1061

Contents lists available at SciVerse ScienceDirect

Talanta

journal homepage: www.elsevier.com/locate/talanta

Short communication

The stable and water-soluble neodymium-doped lanthanide fluoride nanoparticles for near infrared probing of copper ion

Fang-Min Xue, He-Fang Wang *

State Key Laboratory of Medicinal Chemical Biology and Research Center for Analytical Sciences, College of Chemistry, Nankai University, Tianjin 300071, China

ARTICLE INFO

Article history:
Received 12 April 2012
Received in revised form
6 July 2012
Accepted 13 July 2012
Available online 24 July 2012

Keywords:
Lanthanide fluoride
Neodymium
Near infrared
Copper ion

ABSTRACT

Neodymium (Nd^{3+}) doped nanomaterials exhibited the unique near infrared (NIR) luminescence properties. However, the application of Nd-doped nanomaterials to chemosensors was rarely explored. Herein, the water-soluble 2-aminoethyl dihydrogen phosphate stabilized Nd-doped LaF_3 (ADP-Nd-LaF_3) nanoparticles were explored as the NIR probe for chemosensors. The NIR emission intensity at 1061 nm of ADP-Nd-LaF_3 nanoparticles kept stable in the aqueous solution of various pH and coexisting of most common metal ions except copper ion, consequently, the ADP-Nd-LaF_3 nanoparticles were developed as a high selective NIR probe for Cu(II). The NIR emission of ADP-Nd-LaF_3 exhibits a linear quenching response to Cu(II) in the range 5–100 μM, with a detection limit of 0.8 μM. The precision of eleven replicate detections of 5 μM Cu(II) was 0.5% (RSD). The recovery of spiked Cu(II) in human urine and waste water samples ranged from 102 to 109%. The possible mechanism of Cu(II)-induced fluorescence quenching of ADP-Nd-LaF_3 nanoparticles was also discussed.

1. Introduction

Recently, the lanthanide-doped nanomaterials are gaining popularity due to the unique luminescence properties such as superior photostability, large Stoke's shift and long luminescence lifetime [1–5]. Among the numerous lanthanide-doped nanomaterials, neodymium ion (Nd^{3+}) doped nanomaterials have found wide applications in optical cell windows, optical telecommunication windows, and solid-state lasers for their near-infrared (NIR) emission [6–8]. However, to the best of our knowledge, the applications of Nd-doped nanomaterials to the chemo- or biochemo-sensors are seldom reported, although the NIR probes have the merits of the highest tissue-penetrability and the lowest interference from the endogenous fluorescence background [9,10]. The reason behind this is that the emissions of lanthanides are a little sensitive to the chemical environment since their luminescence arises from the well-shielded inner-shell 4f–4f transitions [4,11,12].

Herein, we chose the water-soluble 2-aminoethyl dihydrogen phosphate (ADP) stabilized Nd-doped LaF_3 (ADP-Nd-LaF_3) nanoparticles as the NIR probe to explore the feasibility of the applications of lanthanides-doped nanoparticles to chemosensors. LaF_3 was utilized as the host matrixes owing to the superior optical transparency in the 200–1100 nm region and low vibration energies [7]. ADP was used as the stabilizer to ensure the water-solubility of Nd-doped LaF_3 nanoparticles. Metal ions are chosen as the analytes, since the diverse metal ions are always of great significance [13] and usually have been used as the first examples to explore the applications of the new materials to the field of chemosensors [14–17].

Numerous luminescent materials, such as metal-organic frameworks [16], the specific dyes [17], functionalized quantum dots (QDs) [18–22] and gold nanomaterials [23–25], have been widely investigated for optosensing of the target metal ions. Usually the heavy metal ions such as Cu(II), Cd(II), Hg(II), Pb(II), Co(II), Mn(II), Zn(II), Fe(III), Ni(II), Cr(III), and Ag(I) exhibit diverse effects on the luminescence of QDs [22], resulting in significant interference of the QDs-based probes. However, in the case of ADP-Nd-LaF_3-based NIR probe, most metal ions show little effect on the emission intensity due to the stable luminescence nature against the chemical environment. Consequently, ADP-Nd-LaF_3 nanoparticles have great potential to be the promising high selective probe for chemo-sensing.

Among the most common ions, only copper ion exhibited obvious quenching effect on the NIR emission of ADP-Nd-LaF_3 nanoparticles. So, ADP-Nd-LaF_3 nanoparticles were explored as the potential high selective NIR probe of Cu(II). In fact, optosensing of copper ion has attracted wide interests in recent years, as Cu(II) is an essential trace element in biological systems as well as an important environment pollutant [22–25]. In this paper, the stability of ADP-Nd-LaF_3 nanoparticles in different chemical environment was systematically studied, and the possible mechanism of Cu(II)-induced fluorescence quenching of ADP-Nd-LaF_3 was also discussed.

* Corresponding author.
E-mail address: wanghefang@nankai.edu.cn (H.-F. Wang).

0039-9140/$ - see front matter © 2012 Elsevier B.V. All rights reserved.
http://dx.doi.org/10.1016/j.talanta.2012.07.034

2. Experimental section

2.1. Chemicals

All chemicals used were at least of analytical grade. Ultrapure water (18.2 MΩ cm) was obtained from a Pro water purification system (Labconco Corporation, Kansas City, MO). 2-Aminoethyl dihydrogen phosphate from Sigma-Aldrich was used without further purification. Neodymium nitrate ($Nd(NO_3)_3 \cdot 6H_2O$), tris(hydroxymethyl)aminomethane (Tris), lanthanum nitrate ($La(NO_3)_3 \cdot 6H_2O$), ammonium fluoride (NH_4F) and copper nitrate ($Cu(NO_3)_2 \cdot 3H_2O$) were from Guangfu Fine Chemical Research Institute (Tianjin, China). 4-(2-hydroxyethyl)-1-piperazinee thanesulfonic acid (HEPES) was purchased from Shengong Genetech Co. Ltd (Shanghai, China).

2.2. Instruments

All the steady-state fluorescence and the decay curves were measured on PTI QM/TM/NIR system (Birmingham, NJ), which was equipped a 75W xenon arc lamp and N_2/dyes laser. The absorption spectra were recorded on a UV-3600 UV–vis-NIR spectrophotometer (Shimadzu, Japan). The Fourier transform infrared (FT-IR) spectra (4000-400 cm^{-1}) were recorded on a Magna-560 spectrometer (Nicolet, Madison, WI). High resolution transmission electron microscopic (HR-TEM) images were taken on a Tecnai G2 F20 (Philips, Holland) at 200 kV. The samples for TEM were obtained by drying sample droplets from water dispersion onto a 300-mesh Cu grid coated with a lacey carbon film. The X-ray diffraction (XRD) pattern was recorded with a D/max-2500 diffractometer (Rigaku, Japan) with Cu $K\alpha$ radiation.

2.3. Synthesis of ADP-Nd-LaF_3 nanoparticles

ADP-Nd-LaF_3 nanoparticles were synthesized according to the literature methods [26–28]. Briefly, in a round flask, the solution of 0.111 g (3.00 mmol) NH_4F and 0.144 g (1.02 mmol) ADP in 25 mL of ultrapure water was stirred and heated to 75 °C. Then a solution of $Nd(NO_3)_3 \cdot 6H_2O$ (0.280 g, 0.06 mmol) and $La(NO_3)_3 \cdot 6H_2O$ (0.546 g, 1.26 mmol) dissolved together in 2 mL of water was added dropwise, and the resultant mixture was continuously stirred at 75 °C for 3 h. Finally, the mixture was evaporated to about 4 mL and then the ADP-Nd-LaF_3 nanoparticles were precipitated by the addition of 15 mL acetone and centrifugation. The precipitate was further washed by acetone for three times and dried under vacuum.

2.4. Samples

Human urine samples were collected from the healthy adult volunteers. All the urine samples were centrifuged at 10,000 rpm for 5 min and the supernatants were used for analysis. The waste water samples were collected from local factories and were filtered by 0.45 μm membrane before analysis.

2.5. Fluorescence measurements

The steady-state fluorescence from 800–1400 nm was recorded by high sensitivity TE-cooled InGaAs detector, electronics, lock-in amplifier and chopper built into the lamp housing for noise suppression. The decay curves of fluorescent emission at 1061 nm were recorded with the excitation of 575 nm by exciting the solution of R-590 pumped by a N_2 laser. The lifetime analyses were calculated using the FeliX32 advanced fluorescence software, and were fitted so as to obtain χ^2 values from 0.8 to 1.2. For copper ion determination, the fluorescence was collected in the range of 960–1160 nm upon the excitation of 575 nm with the NIR Hamamastu PMT at voltage −850 V and both the slits of excitation and emission at 24 nm unless special statement. In a 4 mL quartz cell (1 cm × 1 cm), 1 mL of ADP-Nd-LaF_3 nanoparticles (2 g L^{-1}), 1 mL of buffer solution (20 mM) and 20 μL of Cu(II) standard solution or sample solution were mixed thoroughly to get 2 mL solution. The solution was gently shaken before fluorescence measurement.

3. Result and discussion

3.1. Characterization of ADP-Nd-LaF_3 nanoparticles

The prepared ADP-Nd-LaF_3 nanoparticles were characterized by HR-TEM (Fig. S1a and b), XRD (Fig. S1c) and FT-IR (Fig. S1d). The HR-TEM images suggested that the prepared Nd-doped LaF_3 nanoparticles were well dispersed with slight random agglomerations (Fig. S1a). The clear lattice fringes shown in Fig. 1b displayed that the particle sizes were in the range 3–10 nm. The XRD pattern of ADP-Nd-LaF_3 (Fig. S1c) agreed with the data of pure hexagonal LaF_3 crystals [29,30], demonstrating the hexagonal structure of the prepared ADP-Nd-LaF_3. ADP was used as the ligand to control the growth of the nanoparticles and to stabilize the water soluble nanoparticles. To demonstrate the existence of ADP on the surface of nanoparticles, the FT-IR spectra of pure ADP and ADP-Nd-LaF_3 nanoparticles were compared in Fig. S1d. The main vibration bands of ADP such as 2906, 1163, 1085, 1032, 942 and 766 cm^{-1} were also observed in the FT-IR spectrum of

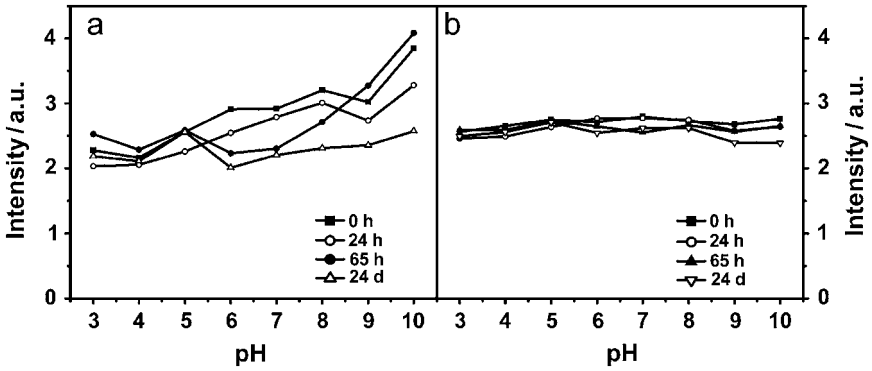

Fig. 1. Emission intensity at (a) 890 nm and (b) 1061 nm of 1 g L^{-1} ADP-Nd-LaF_3 nanoparticles in different pH buffer solution during different time. Data were recorded by high sensitivity TE-cooled InGaAs detector with both the slits of emission and excitation at 24 nm. pH 3.0–5.0 was buffered by 10 mM acetate solution and pH 6.0–10.0 was buffered by 10 mM Tris–HCl solution.

ADP-Nd-LaF_3 nanoparticles. The absorption band at 1636 cm^{-1} was assigned to O–H vibration due to the chemically bonded or physically absorbed water onto the surface of the nanoparticles.

3.2. Fluorescence spectra and stability of ADP-Nd-LaF_3 nanoparticles

The emission peaks (Fig. S2a) of ADP-Nd-LaF_3 nanoparticles at 890, 1061, and 1260 nm agree well with the typical Nd^{3+} transitions of $^4F_{3/2}\rightarrow{}^4I_{9/2}$, $^4F_{3/2}\rightarrow{}^4I_{11/2}$ and $^4F_{3/2}\rightarrow{}^4I_{13/2}$, respectively. The characteristic emission of 1061 nm can be excited by several bands such as 350, 514, 575, 735 and 792 nm, with the highest excitation efficiency at 575 nm (Fig. S2b).

The prepared ADP-Nd-LaF_3 nanoparticles display good stability as elucidated by the little variation of the fluorescence intensity against the pH of the aqueous solution of ADP-Nd-LaF_3 during different time (Fig. 1). The emission at 1061 nm was nearly independent of the pH, and the fluorescence intensity at each pH remained stable for 20 days (Fig. 1b). The emission intensity at 890 nm, however, exhibited larger variations against pH during different time (Fig. 1a). We chose the 1061 emission for the subsequent investigations. The emission of Nd^{3+} came from the transitions inside the $4f^4$ shell, which was well shielded from the chemical environment by the closed $5s^2$ and $5p^6$ shells, thus the external environment (such as pH) can only perturb the electronic configurations to a limited extent, resulting in the good stability of ADP-Nd-LaF_3 nanoparticles in different pH environment.

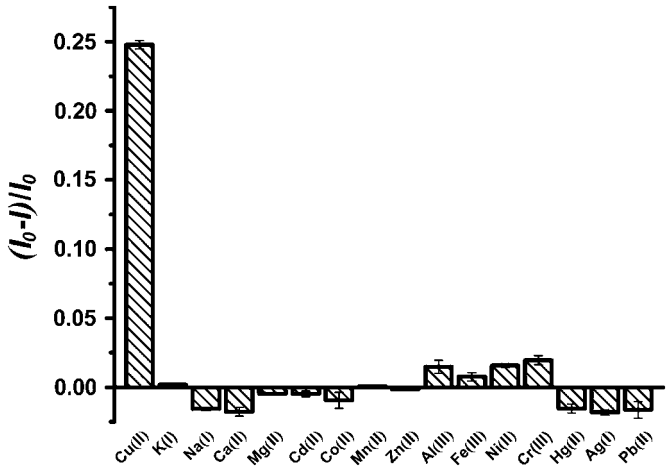

Fig. 2. Quenching percent of 1 g L^{-1} ADP-Nd-LaF_3 nanoparticles by 50 μM Cu(II), 10 mM K(I), Na(I), Ca(II), Mg(II), Cd(II), 1 mM Co(II), Mn(II) and 500 μM Zn(II), Al(III), Fe(III), Ni(II), Cr(III), Hg(II), Ag(I), Pb(II) buffered by 10 mM HEPES solution (pH 7.4). All emission intensity was monitored at 1061 nm upon the excitation of 575 nm with the NIR Hamamastu PMT at voltage −850 V and both the slits of emission and excitation at 24 nm.

In addition, the ADP-Nd-LaF_3 nanoparticles also display good stability against different metal ions except copper ion (Fig. 2). The emission intensity at 1061 nm of ADP-Nd-LaF_3 shows less than 2% variations upon the addition of 10 mM of K(I), Na(I), Ca(II), Mg(II), Cd(II), 1 mM of Co(II), Mn(II) and 500 μM of Zn(II), Al(III), Fe(III), Ni(II), Cr(III), Hg(II), Ag(I) and Pb(II). However, the addition of 50 μM of Cu(II) causes about 25% quenching of emission intensity at 1061 nm. So, further investigations focused on exploring of ADP-Nd-LaF_3 nanoparticles as the NIR probes for Cu(II) and the possible reasons for the large quenching effect of Cu(II) on the NIR emission of ADP-Nd-LaF_3 nanoparticles.

3.3. Detection of Cu(II) by ADP-Nd-LaF_3 NIR probe

Although the emission intensity at 1061 nm of ADP-Nd-LaF_3 nanoparticles was independent on the variations of pH (Fig. 1b), the interaction between the copper ion and ADP-Nd-LaF_3 nanoparticles was pH dependent (Fig. 3a). The highest quenching efficiency of the two buffer systems involved, i.e., HEPES and Tris–HCl, were both observed at pH 7.4. The quenching efficiency in HEPES buffer was all higher than that in Tris–HCl buffer, and there was a platform from pH 7.0 to 7.4 when HEPES was used to buffer the system. The reasons behind the above-mentioned facts were that the existing state of Cu(II) and the charge state of ADP attached on the surface of ADP-Nd-LaF_3 nanoparticles were all related with pH value and the kind of buffer. Higher pH led to the precipitation of copper ion, and thus the lower quenching efficiency; however, lower pH resulted in the protonation of the amino group of ADP, and thus the weaker binding of Cu(II) to the amino group of ADP, and finally cause the lower quenching efficiency. As the kind of buffer was concerned, the amino groups of Tris competed with amino groups of ADP attached on the surface of ADP-Nd-LaF_3 to bind with Cu(II), resulting in the lower quenching efficiency in Tris–HCl buffer. Consequently, the HEPES buffer at pH 7.4 was chosen as the media in most part of this paper.

The interaction of ADP-Nd-LaF_3 nanoparticles and copper ions was very rapid and the quenched signal was also very stable (Fig. 3b). The fluorescence quenching of ADP-Nd-LaF_3 by copper ion reached the maximum efficiency within 1 min, and kept stable in the subsequent 26 min.

To demonstrate the feasibility of ADP-Nd-LaF_3 NIR probe for the detection of copper ion, the fluorescence spectra of 1 g L^{-1} ADP-Nd-LaF_3 nanoparticles in the absence and presence of copper ion were recorded in 10 mM HEPES (pH 7.4) buffer (Fig. 4a). The gradually reduced emission intensity at 1061 nm was observed upon the increase of concentration of copper ion (C_{cu}). In the range 5–100 μM, the linear relationship of the quenched efficiency ($\Delta I/I_0$ at 1061 nm against the C_{cu} was observed with the

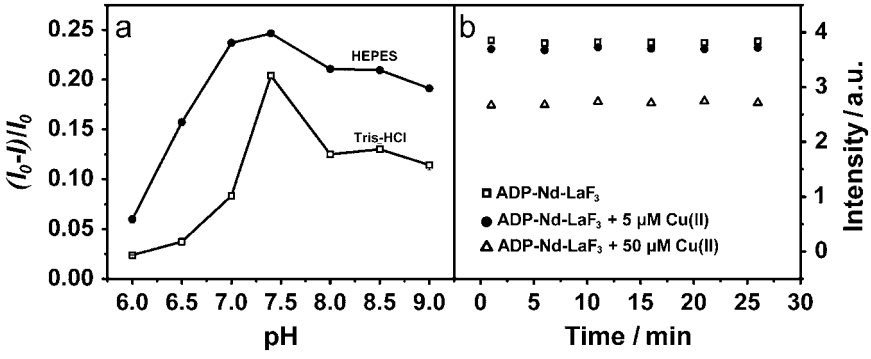

Fig. 3. (a) pH-dependent quenching efficiency of 50 μM Cu(II) to the emission intensity at 1061 nm of 1 g L^{-1} ADP-Nd-LaF_3 in 10 mM HEPES or Tris–HCl buffer solutions; (b) the time frame of the interaction of Cu(II) and 1 g L^{-1} ADP-Nd-LaF_3 nanoparticles in 10 mM HEPES buffer (pH 7.4). Conditions were as Fig. 2.

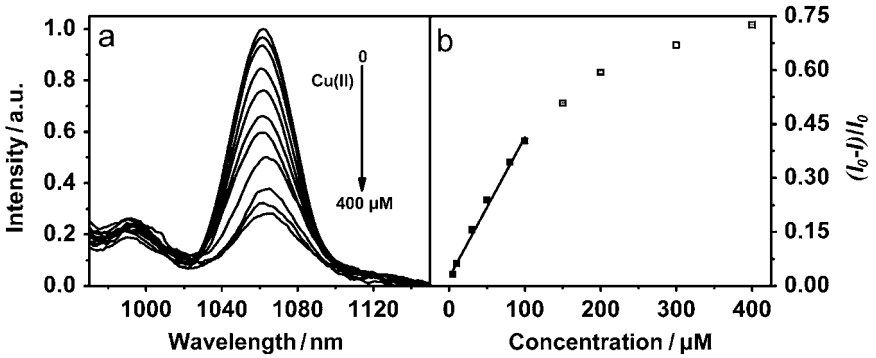

Fig. 4. Fluorescence response of 1 g L^{-1} ADP-Nd-LaF_3 to copper ion in 10 mM HEPES buffer (pH 7.4): (a) the fluorescence spectra; (b) the linear plot of quenching percent at 1061 nm against the concentration of copper ion. Conditions were as Fig. 2.

calibration function $\Delta I/I_0 = 0.00389C_{Cu} + 0.02398$ (where C_{Cu} is in μM) and a correlation coefficient of 0.9939 (Fig. 4b). The precision of eleven replicate detections of 5 μM Cu(II) was 0.5% (relative standard deviation, RSD). The detection limit (DL) calculated as the C_{cu} which produced a quenched efficiency three times the standard deviation of the blank signal, was 0.8 μM.

To further evaluate the selectivity of ADP-Nd-LaF_3-based NIR probe for Cu(II) detection, the interference of co-existing ions are examined (Fig. S3). The quenching efficiency of 50 μM Cu(II) was not unaffected by 10 mM of K(I), Na(I), Ca(II) and Mg(II), 1 mM of Cd(II), Mn(II), Co(II), Ni(II), Ag(I), Zn(II) and Al(III). The tolerance of Fe(III), Cr(III), Hg(II) and Pb(II) was 200 μM.

To find the potential application of the developed method, ADP-Nd-LaF_3 NIR probe was employed for the detection of Cu(II) in human urine and waste water samples. As the content of Cu(II) in these samples was below the DL of the developed method, a spike-recovery test was performed. As shown in Table S2, the recovery of spiked Cu(II) in these samples ranged from 102 to 109%.

3.4. Possible mechanism of Cu(II)-induced fluorescence quenching of ADP-Nd-LaF_3

To explore the possible mechanism of Cu(II)-induced fluorescence quenching of ADP-Nd-LaF_3, three experiments were explored including the spectral overlap, fluorescence restoration, and life time measurements.

Fig. S4a and b show the spectral overlap between the absorption spectra of the metal ions and the emission spectrum of ADP-Nd-LaF_3 nanoparticles. Cu(II) has wide absorbance in the range 500–1200 nm (with the maximum at 710 nm), and exhibits large red-shift to 575–1200 nm (with the maximum at 810 nm) upon the addition of ADP, suggesting the charge transfer of Cu (II) to ADP (Fig. S4a). Note that ADP has the terminal amino group, which acts as the binding site of Cu(II) to ADP-Nd-LaF_3 [31]. Furthermore, the broad spectral overlap between the emission spectrum of ADP-Nd-LaF_3 and the absorption spectrum of Cu(II)/Cu(II)–ADP complex was observed (Fig. S4a). While other ions used in this paper did not display obvious absorbance at 600–1200 nm in the absence and presence of ADP (Fig. S4b). So, the most possible reason of Cu(II)-induced fluorescence quenching of ADP-Nd-LaF_3 was the charge transfer and fluorescence resonance energy transfer (FRET) between the Cu(II) and ADP-Nd-LaF_3 through the binding of Cu(II) to the amino group of ADP attached on the surface of ADP-Nd-LaF_3 nanoparticles and the spectral overlap between the absorption spectrum of Cu(II)/Cu(II)–ADP complex and the emission spectrum of ADP-Nd-LaF_3.

The charge transfer and FRET between Cu(II) and ADP-Nd-LaF_3 was also proven by the pH-dependent quenching efficiency in Fig. 3a. In lower pH, the amino groups were protonated, and the binding of Cu (II) to the protonated ADP would definitely weakened, thus leading to the weaker charge transfer or the increased distance between Cu (II) and ADP-Nd-LaF_3, and finally resulting in the lower quenching efficiency in lower pH environment. Such properties make ADP-Nd-LaF_3-Cu system have great potential for indicating the growth of cancer as the decreased pH from 7.4 to 6.0 are always associated with cancers [32].

Although the wide absorbance of Cu(II) and Cu(II)–ADP complex was also in the range of the excitation spectrum of ADP-Nd-LaF_3 (Fig. S4c), the contribution of the inner-filter effect to the Cu(II)-induced fluorescence quenching of ADP-Nd-LaF_3 was not reasonable. As elucidate by the quenching efficiency measured at different excitation wavelengths in Fig. S4d, the highest quenching efficiency was achieved at the excitation of 575 nm, however, the absorbance of Cu(II)/Cu(II)–ADP at 575 nm was much lower than that at 735 and 792 nm. Moreover, the absorbance of Fe(III) at 575 nm was higher than that of Cu(II) (Fig. S4b), while the quenching efficiency of Fe(III) was much lower than that of Cu(II) (Fig. 2).

The Cu(II)-induced fluorescence quenching of ADP-Nd-LaF_3 was the dynamic quenching process, as the relationship of I_0/I and the concentration of Cu(II) (C_{Cu}) agreed well with the Stern–Volmer equation (Fig. S5a). The linear function of I_0/I and C_{Cu} was $I_0/I = 0.00667\ C_{Cu} + 1$ (I_0 and I refer to fluorescence intensity in the absence and the presence of certain C_{Cu} in μM) with $R^2 = 0.9998$ and $K_{SV} = 6670\ M^{-1}$. Furthermore, the fluorescence lifetime of ADP-Nd-LaF_3 exhibited obvious decrease in the presence of Cu(II) (Fig. S5b and Table S2).

4. Conclusions

We have evaluated the stability of ADP-Nd-LaF_3 nanoparticles in various environments including various pH and coexisting of the most common metal ions. Among those metal ions, only Cu(II) exhibited fluorescence quenching to the NIR emission of ADP-Nd-LaF_3 nanoparticles. The possible mechanism for Cu(II)-induced dynamic fluorescence quenching of ADP-Nd-LaF_3 was the charge transfer and FRET between Cu(II) and ADP-Nd-LaF_3 nanoparticles. Although the DL of the ADP-Nd-LaF_3-based NIR probe for Cu(II) detection still need to be improved, the data presented in this paper will be helpful for further understanding of the luminescent property of rare-earth nanoparticles and will put forward the application of the rare-earth nanoparticles to the high sensitive and selective sensors.

Acknowledgements

This work was supported by the National Basic Research Program of China (no. 2011CB707703), the National Natural Science

Foundation of China (nos. 20935001, 20977049, 21175073) and the Fundamental Research Funds for the Central Universities.

Appendix A. Supporting information

Supplementary data associated with this article can be found in the online version at http://dx.doi.org/10.1016/j.talanta.2012.07.034.

References

[1] J. Shen, L.D. Sun, C.H. Yan, Dalton Trans. (2008) 5687–5697.
[2] K. Binnemans, Chem. Rev. 109 (2009) 4283–4374.
[3] J.C.G. Bünzli, Chem. Lett. 38 (2009) 104–109.
[4] J.C.G. Bünzli, Chem. Rev. 110 (2010) 2729–2755.
[5] S.V. Eliseeva, J.C.G. Bünzli, Chem. Soc. Rev. 39 (2010) 189–227.
[6] X.X. Cui, J.B. She, K. Cui, C. Gao, C.Q. Hou, W. Wei, B. Peng, Chem. Phys. Lett. 489 (2010) 191–194.
[7] X.X. Cui, J.B. She, C. Gao, K. Cui, C.Q. Hou, W. Wei, B. Peng, Chem. Phys. Lett. 494 (2010) 60–63.
[8] J.W. Stouwdam, F. van Veggel, Nano Lett. 2 (2002) 733–737.
[9] H. Qian, C. Dong, J. Peng, X. Qiu, Y. Xu, J. Ren, J. Phys. Chem. C. 111 (2007) 16852–16857.
[10] H.C. Pan, R.J. Cui, J.J. Zhu, J. Phys. Chem. B. 112 (2008) 16895–16901.
[11] P. Dorenbos, J. Lumin. 91 (2000) 155–176.
[12] P. Dorenbos, J. Lumin. 91 (2000) 91–106.
[13] J.H. Jung, J.H. Lee, S. Shinkai, Chem. Soc. Rev. 40 (2011) 4464–4474.
[14] H.N. Kim, Z.Q. Guo, W.H. Zhu, J. Yoon, H. Tian, Chem. Soc. Rev. 40 (2011) 79–93.
[15] D.L. Ma, D.S.H. Chan, B.Y.W. Man, C.H. Leung, Chem.-Asian J. 6 (2011) 986–1003.
[16] J. Rocha, L.D. Carlos, F.A.A. Paz, D. Ananias, Chem. Soc. Rev. 40 (2011) 926–940.
[17] J.F. Zhang, Y. Zhou, J. Yoon, J.S. Kim, Chem. Soc. Rev. 40 (2011) 3416–3429.
[18] Y.F. Chen, Z. Rosenzweig, Anal. Chem. 74 (2002) 5132–5138.
[19] R. Freeman, T. Finder, I. Willner, Angew. Chem. Int. Ed. 48 (2009) 7818–7821.
[20] P. Wu, Y. Li, X.-P. Yan, Anal. Chem. 81 (2009) 6252–6257.
[21] P. Zrazhevskiy, M. Sena, X.H. Gao, Chem. Soc. Rev. 39 (2010) 4326–4354.
[22] Q.G. Chen, T.Y. Zhou, C.Y. He, Y.Q. Jiang, X. Chen, Anal. Methods 3 (2011) 1471–1474.
[23] Y. Zhou, S.X. Wang, K. Zhang, X.Y. Jiang, Angew. Chem. Int. Ed. 47 (2008) 7454–7456.
[24] C.V. Durgadas, C.P. Sharma, K. Sreenivasan, Analyst 136 (2011) 933–940.
[25] J.-M. Liu, H.-F. Wang, X.-P. Yan, Analyst 136 (2011) 3904–3910.
[26] P.R. Diamente, F. van Veggel, J. Fluoresc. 15 (2005) 543–551.
[27] P.R. Diamente, R.D. Burke, F. van Veggel, Langmuir 22 (2006) 1782–1788.
[28] C.H. Dong, M. Raudsepp, F. van Veggel, J. Phys. Chem. C. 113 (2009) 472–478.
[29] F. Wang, Y. Zhang, X.P. Fan, M.Q. Wang, Nanotechnology 17 (2006) 1527–1532.
[30] L.J. Charbonniere, J.L. Rehspringer, R. Ziessel, Y. Zimmermann, New J. Chem. 32 (2008) 1055–1059.
[31] L. Mazurowska, K. Nowak-Buciak, M. Mojski, Anal. Bioanal. Chem. 388 (2007) 1157–1163.
[32] L. Frullano, C. Catana, T. Benner, A.D. Sherry, P. Caravan, Angew. Chem. Int. Ed. 49 (2010) 2382–2384.